Agricultural Sciences, 2026, 17(3), 219-242
https://www.scirp.org/journal/as
ISSN Online: 2156-8561
ISSN Print: 2156-8553

Development of Halloysite-Stabilized Neem Oil Emulsions: A Greener Formulation Strategy for Agricultural Pest Management

Sandeep S. Palkhe[1*], Mayur A. Patil[2], Gunvant H. Sonawane[3]

[1]Department of Chemistry, Arts, Commerce and Science College Dharangaon, Jalgaon, India
[2]Department of Chemistry, Dadasaheb Sureshji Patil College Chopda, Jalgaon, India
[3]Department of Chemistry, KVPS Arts, Commerce and Science College Parola, Jalgaon, India
Email: *palkhess@rediffmail.com, drgunvantsonawane@gmail.com

How to cite this paper: Palkhe, S.S., Patil, M.A. and Sonawane, G.H. (2026) Development of Halloysite-Stabilized Neem Oil Emulsions: A Greener Formulation Strategy for Agricultural Pest Management. *Agricultural Sciences*, **17**, 219-242.
https://doi.org/10.4236/as.2026.173014

Received: January 19, 2026
Accepted: March 21, 2026
Published: March 24, 2026

Abstract

Developing an Eco-friendly formulation is essential to reducing the use of traditional pesticides. Halloysite nanotubes were added as a stabilizing or emulsifying agent, neem oil was utilized to create Pickering emulsions, and acephate was added to evaluate the pesticidal effectiveness. Microscopic images show that the interfacial tension and droplet size decrease with increasing HNT levels. The contact angle affects the pesticide formulations' capacity to stick, moisten, and disperse on plant leaves. The majority of produced emulsions exhibit good wettability at contact angles below 60˚. HNTs were efficiently adsorbed at droplet interfaces, as confirmed by EDS, SEM, and FTIR, ensuring the stability of the emulsion. *Escherichia coli*, *Pseudomonas aeruginosa*, *Bacillus cereus*, and *Staphylococcus aureus* were the bacterial strains employed to test the biosafety. Using *Spodoptera frugiperda* as a pest model and maize as a plant model, insecticidal tests were conducted. It is neem oil-based emulsions that have the highest fatality rate. These results show that HNT-stabilized Neem oil emulsions provide a reliable, environmentally friendly, and biosafe platform for pest control.

Keywords

Neem Oils, Halloysites, Acephate, *Spodoptera frugiperda*, Emulsion Stability

1. Introduction

The population of the world is increasing daily at a rapid pace. Over the next three decades, this will result in a 70% increase in food demand [1] [2]. Despite the green revolution, pests and diseases have had a significant impact on crop pro-

duction [3] [4]. Use of agrochemicals, such as pesticides, is crucial to resolving this problem. However, overuse of conventional pesticides causes major problems for the environment and human health, including non-target toxicity, pesticide residues, and pest resistance [5]. Reducing the detrimental effects of pesticides on the environment and other non-target organisms is crucial. This can be accomplished by employing formulations with controlled release [6]. An important application of the CRF system is that it reduces the location of pests in the field by optimizing the required doses compared to the traditional method of administration [7] [8]. In addition, CRFs demonstrate reliable and reproducible delivery of the drug to the target area over the required length of time with prolonged effects. Pickering emulsion is the important form of controlled release formulations. Pickering emulsions can be either inverse (water-in-oil) or oil-in-water (o/w) emulsions [9]-[11]. Pickering emulsion offers many benefits over conventional emulsion, including lower costs, less toxic effects, increased stability, and environmental friendliness [12]. Today, nanocontainers are widely used to manufacture various CRFs. Nanocontainers can be roughly divided into two types: a) Polymer nanocontainers, b) Inorganic Nanocontainers (Porous inorganic materials). Nanoparticles (NPs) that self-assemble at the oil/water interface and function as a physical barrier stabilize Pickering emulsions. The nano pesticides developed by using nanocontainers can increase water solubility, bioavailability and protect agrochemicals against environmental degradation [13], at the same time it can control pathogens, weeds, and insects in the crops1 [14]-[16]. Rod-like nanoparticles have many benefits, including high emulsion stability, minimal environmental pollution, and low toxic effects. Pickering emulsion stabilized by these nanomaterials has therefore garnered a lot of interest. Halloysites nanotubes (HNTs) are one type of rod-like nanomaterial; they have a tubular structure, a large length: diameter ratio, and active hydroxyl groups on their surfaces [17]. As a result, HNTs can serve as an anchor point for molecular adsorption and grafting reactions [18]. Additionally, HNTs are biocompatible and environmentally benign materials that can be utilized in nearly any application [19]-[21]. The majority of earlier research used organic solvents to prepare Pickering emulsions, which have negative impacts on both the environment and human health [22]. Therefore, when making such emulsions, safer solvents like natural oils should be taken into account [23]. Neem oil is among these safer natural oils. Azadirachtin is the active ingredient in the neem tree (*Azadirachta indica*), which is categorized as an antifeedant. It is mostly found within neem seeds. Neem seed kernels contain approximately 0.2% to 0.8% azadirachtin by weight, whereas neem oil can account for 30% to 50% of the total weight of the seeds. Azadirachtin functions as an insect poison because it can interfere with the synthesis of the hormone ecdysone, which causes the insects to wither and eventually die [9]. Additionally, azadirachtin has the ability to obstruct and suffocate insects' breathing pores. As a result, pesticide contact activity is crucial. Although numerous studies have been conducted on neem oil and Pickering emulsion systems. But very little research has been done on combina-

tion of neem oil-based Pickering emulsions stabilized by halloysite nanotubes for multipurpose pest control applications.

In this work, neem oil was used to prepare O/W emulsions. Following the addition of HNT as an emulsifying agent, emulsion stability was assessed. As the HNT concentration rises, the water-neem oil emulsion becomes more stable. HNTs-Acephate O/W emulsions were then made by combining acephate with HNT aqueous dispersions. The HNTs-Acephate O/W emulsions have good stability because the adsorption and aggregation of HNTs at the oil droplet interface creates a three-dimensional network structure that prevents emulsion aggregation. Cotton and maize were used as the plant models and *S. frugiperda* as the pest model to assess the insecticidal activity of HNTs-Acephate emulsions. To assess the biosafety of these emulsions, the effects of various HNTs-acephate emulsion concentrations on the bacteria *Pseudomonas aeruginosa*, *Bacillus cereus*, *Escherichia coli*, and *Staphylococcus aureus* were investigated (Figure 1).

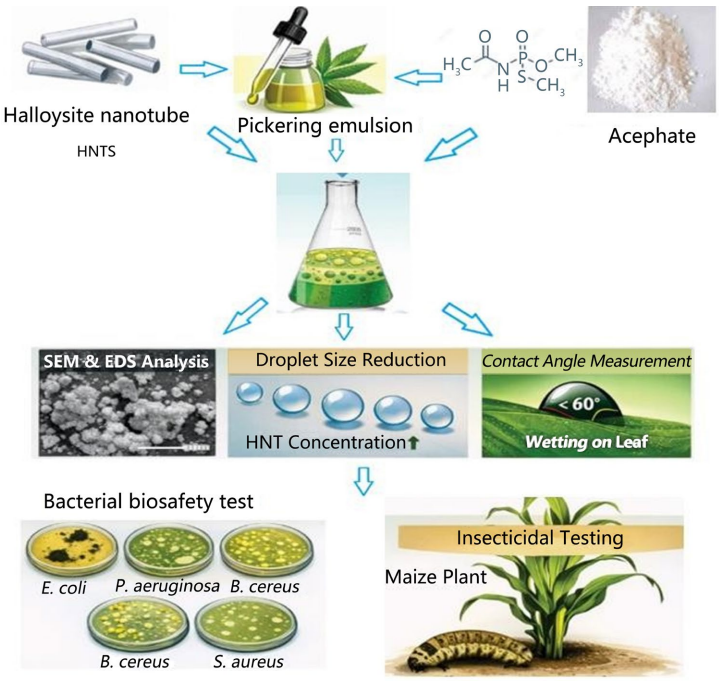

Figure 1. Graphical abstract.

2. Experimental Section

2.1. Materials and Methods

Sigma-Aldrich India supplied the halloysite nanotubes (HNTs). Neem oil was obtained using the cold press process. Acephate was obtained from Rallies India Pvt. Ltd. Fresh cotton (Gossypium) and maize (Zea mays) leaves were obtained from the Jalgaon area of Maharashtra, India. Deionized water was utilized in all of the trials. Fourier transform infrared (FT-IR) spectra were recorded using FT-FTIR affinity model no. 1 with 2.0 cm^{-1} resolution in the 4000 - 400 cm^{-1} range. Microscopic images of Pickering emulsions were captured using a Bio Mini IS 4381 dig-

ital microscopes at 40 X magnification. The contact angle analyzer (DSA 100, Data Physics, OCA-25, Germany) was used to measure the droplet contact angle on the leaf surface. The vacuum freeze drier FDL2-10N -2-60 B was utilized, with the temperature set at −55˚. High Speed homogenizer (Remi RQ-127 A/D) was used for homogenization.

2.2. Preparation of HNTs-Neem Oil Emulsion

Pickering emulsion is prepared in two steps. It is described in Figure 2. In first step Pickering emulsions were created by homogenizing and sonicating an aqueous solution of neem oils for 20 minutes at 1:9, 2:8, and 3:7 oil/water volume ratios. To stabilize Pickering emulsions, different amounts of HNTs (0, 0.5, 1, 2, and 5 weight percent) were added in it.

2.3. Preparation of HNTs-Acephate-Neem Oil Emulsion

A pesticide inserted Pickering emulsions were created by adding 0.5 g of Acephate to previously prepared Pickering emulsions at various concentrations (0, 0.5, 1, 2, and 5 wt%) of HNTs, homogenizing, and sonicating for 20 minutes.

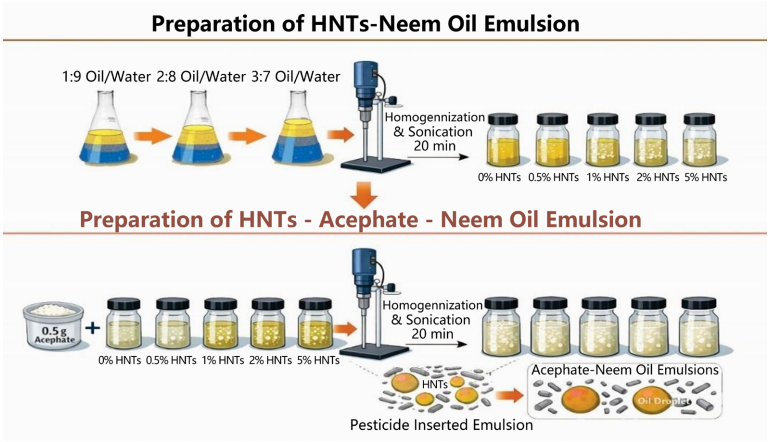

Figure 2. Preparation of Neem oil-based Pickering emulsion.

2.4. Characterization

Microscopic images of Droplets of Various Neem oil-based Pickering emulsion

Droplet size depends upon interfacial tension. Lower the interfacial tension, smaller is the droplet size and *vice versa* [3]. Here for these emulsions, HNT reduces interfacial tension, which in turn reduces droplet size. Emulsions with smaller droplets are more likely to exhibit kinetic stability. Smaller droplet sizes usually result in greater stability. This is because smaller droplets have a higher surface area to volume ratio, which makes it easier for stabilizing particles to be adsorbed at the interface. Figure 3 represents the microscopic images of Droplets of Various Neem oil-based Pickering emulsion. Halloysite nanotubes adsorb at the oil-water interface in the previous Pickering emulsions, creating a rigid barrier. Compared to surfactants, this barrier inhibits droplet coalescence far more

effectively. Neem oil Samples A, B, and C represent Pickering emulsions according to the oil to water ratio. For samples A, B, and C, the corresponding O/W ratios are 2:8, 3:7, and 1:9 Sample A exhibits greater stability and smaller droplets at HNT concentrations of 0.2% and 0.5%. In contrast, Sample B, which contains 0.1% and 0.2% HNT, has more stability and smaller droplets. While, Sample C, which has a 0.2% HNT content, exhibits the smallest droplets and the highest stability. As a result amongst all these samples, the sample containing 0.2% HNT show smallest droplet size and maximum stability. Therefore, the stability of the Pickering emulsion will increase with the HNT content. A Digital Binocular Microscope (Micron optic) was used to study droplet images of these emulsions at magnifications ranging from 4x to 100x. A digital micro imaging camera manufactured by Micaps Ltd. was used to take microscopic pictures.

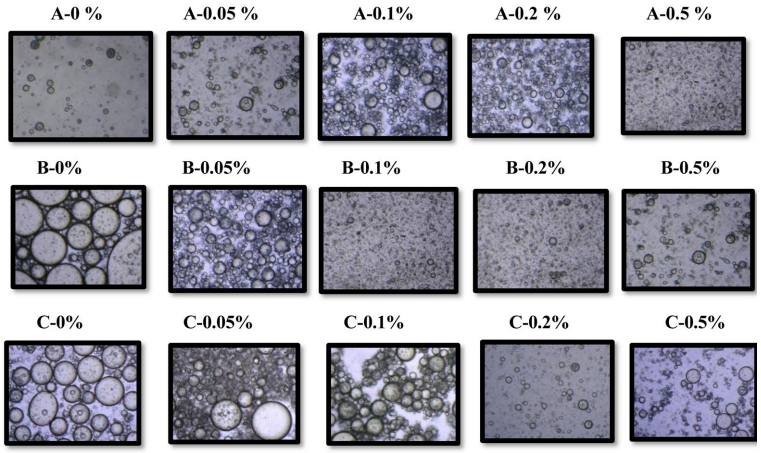

Figure 3. Microscopic images of Droplets of Various Neem oil -based Pickering emulsion.

Antimicrobial activity of Pickering emulsions prepared by using Neem oil - Methodology

The cultures *Staphylococcus aureus, Bacillus cereus*, *Pseudomonas* sp., and *Escherichia coli* were grown in nutrient broth medium. The nutrient broth medium was purchased from "HI Media Laboratories, Mumbai". The Nutrient broth composition was (g/l) Peptone 10.0 Beef extract 10.0, Sodium chloride 5.0, pH after sterilization 7.3 ± 0.1. It was grown at 37˚C for its accelerated growth. Freshly grown culture was spread on the nutrient agar plate. A well 0.7 mm diameter with sterile borer was prepared in the medium. Each sample having a varied concentration each 100 µl (microliter) was loaded to well in plate. Plates were incubated at 37˚C and observed for growth of that respective microorganism on plate. After incubation, the zone of inhibition was checked around the colony and its diameter were measured.

Controls:

Negative control: Sterile distilled water and blank Pickering emulsion (without neem oil).

Positive control: Streptomycin (10 µg/mL) solution.

The zone of inhibition data obtained from antimicrobial assays were analyzed using one-way analysis of variance (ANOVA) to determine significant differences among treatment concentrations and formulation types. The antimicrobial activity of neem oil-based Pickering emulsions prepared at different oil-to-water (O/W) ratios (2:8, 3:7, and 1:9) was evaluated against Gram-positive and Gram-negative bacterial strains including *Staphylococcus aureus*, *Bacillus cereus*, *Escherichia coli*, and *Pseudomonas aeruginosa* using the agar well diffusion method. Test samples and its control against different bacteria is demonstrated.

Results:

Sample A (2 + 8 O/W ratio): Table 1 describes the zone of inhibition, while Figure 4 shows a graphical representation of sample A against various bacterial strains.

Staphylococcus aureus: The zone of inhibition significantly increased from 1.2 cm at 0% concentration to 1.4 cm at both 1% and 2% concentrations. This indicates a positive correlation between concentration and antimicrobial activity.

Bacillus cereus: The inhibition zone increased from 0.9 cm to 1.4 cm at 2%, suggesting moderate activity.

***Pseudomonas* sp.:** No significant antimicrobial activity was observed across all concentrations (0%, 0.05%, and 2%), indicating resistance.

Escherichia coli: A notable increase in the zone of inhibition was recorded, from 0.8 cm at 0% to 1.35 cm at 1% and subsequently decreasing to 1.2 cm at 2%.

Table 1. Zone of inhibition for Sample-A.

Sr. No.	Sample	Percent	Zone of inhibition			
			S. aureus	*B. cereus*	*Pseudomonas* sp.	*E. coli*
1	8 + 2	0%	1.2	0.9	0.8	0.8
2	8 + 2	0.05%	1.35	0.8	0.8	0.85
3	8 + 2	1%	1.4	1.2	0	1.35
4	8 + 2	2%	1.4	1.4	0.8	1.2
5	8 + 2	5%	1.3	0.9	0	0.9

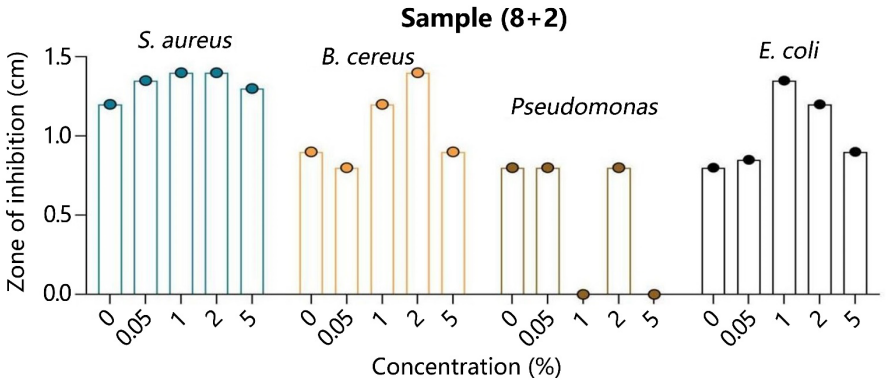

Figure 4. Graphical representation of zone of inhibition for Sample-A.

Sample B (3 + 7 O/W ratio): Table 2 describes the zone of inhibition, while Figure 5 depicts a graphical representation of sample B against numerous bacterial strains.

Staphylococcus aureus: A consistent increase in the zone of inhibition was observed, peaking at 1.65 cm at the 5% concentration.

Bacillus cereus: The inhibition remained relatively constant (0.8 cm) across most concentrations, except for a slight increase at the 5% concentration.

***Pseudomonas* sp.:** Inhibition was noted only at concentrations of 0%, 0.05%, and 5%, while no activity was observed at 1% and 2%.

Escherichia coli: The highest zone of inhibition (1.5 cm) was recorded at the lowest concentration (0.05%), indicating significant activity compared to other samples.

Table 2. Zone of inhibition for Sample-B.

Sr. No.	Sample	Percent	Zone of inhibition			
			S. aureus	*B. cereus*	*Pseudomonas*	*E. coli*
1	7 + 3	0%	1.5	0.8	0.9	1.3
2	7 + 3	0.05%	1.2	1	1.1	1.5
3	7 + 3	1%	1.3	0.8	0	0.9
4	7 + 3	2%	1.5	0.8	0	1.2
5	7 + 3	5%	1.65	0.8	0.9	1

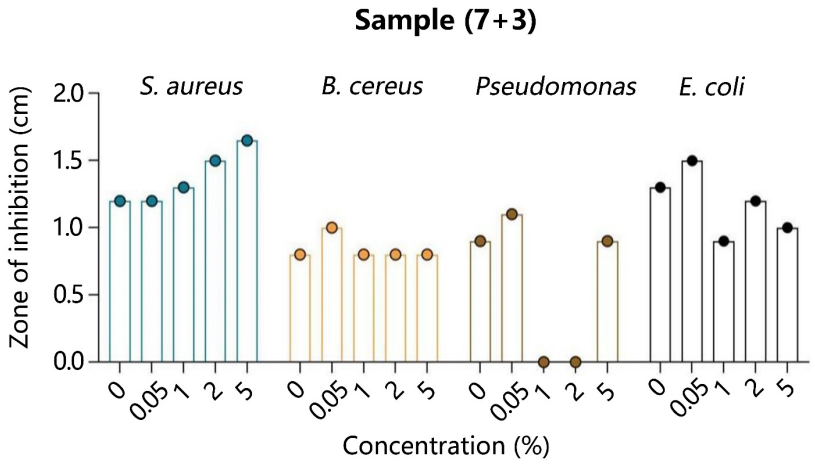

Figure 5. Graphical representation of zone of inhibition for Sample-B.

Sample C (1 + 9 O/W ratio): Table 3 describes the zone of inhibition, while Figure 6 depicts a graphical representation of sample C against numerous bacterial strains.

Staphylococcus aureus: The zone of inhibition showed an increasing trend from 1.3 cm at 0% to a peak of 2 cm at the 2% concentration, followed by a decrease at the highest concentration (5%).

***Bacillus cereus*:** Moderate antimicrobial activity was observed, with an inhibition zone of up to 1 cm.

***Pseudomonas* sp.:** Similar to sample 8 + 2, there was no significant activity noted except for concentrations of 0%, 1%, and 5%.

***Escherichia coli*:** Moderate activity was observed with a maximum zone of inhibition of approximately 1.2 cm.

Table 3. Zone of inhibition for Sample-C.

Sr. No.	Sample	Percent	Zone of inhibition			
			S. aureus	*B. cereus*	*Pseudomonas*	*E. coli*
1	9 + 1	0%	1.3	0.9	0.9	1.1
2	9 + 1	0.05%	1.4	0.8	0	0.8
3	9 + 1	1%	1.5	0.95	1.1	1.1
4	9 + 1	2%	2	0.7	0	0.8
5	9 + 1	5%	1.6	1	1.3	1.2

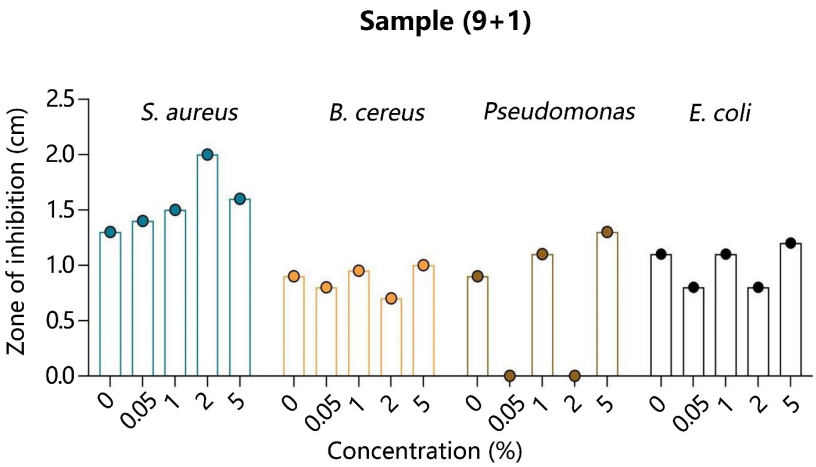

Figure 6. Graphical representation of zone of inhibition for Sample-C.

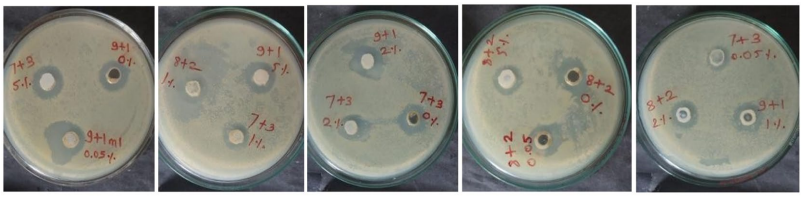

(a)

(b)

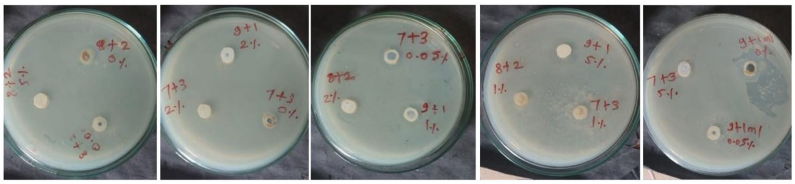

(c)

(d)

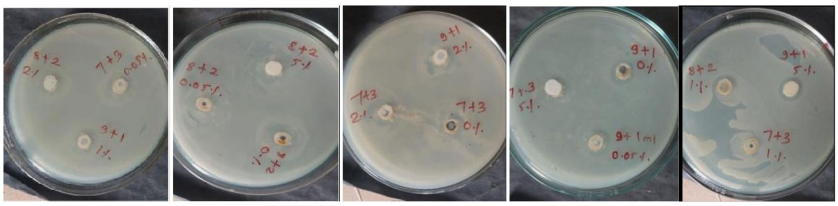

(e)

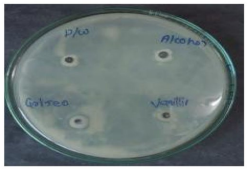

(f)

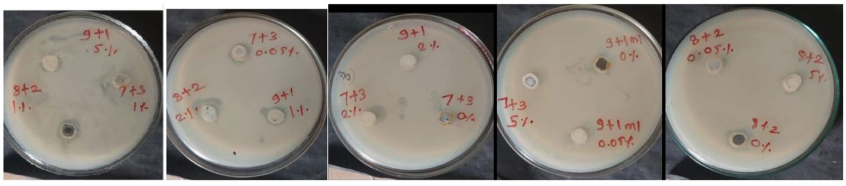

(g)

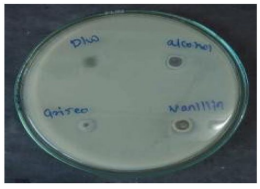

(h)

Figure 7. Antibacterial activity against various bacterial strain, (a) Test samples for *Staphylococcus aureus*; (b) Control for *Staphylococcus aureus*; (c) Test samples for *Pseudomonas aeruginosa*; (d) Control for *Pseudomonas aeruginosa*; (e) Test samples for *E. coli*; (f) Control for *E. coli*; (g). Test samples for *Bacillus cereus*; (h) Control for *Bacillus cereus*.

Conclusion: When compared to control groups: Sample 8 + 2 demonstrated high antimicrobial activity against *S. aureus* at concentrations of 0.05%, 1%, and 2%. For *Bacillus cereus*, significant activity was noted only at concentrations of

1% and 2%. Sample 7 + 3 exhibited higher antimicrobial efficacy against *S. aureus* and *E. coli* specifically at concentrations of 2% and above. Sample 9 + 1 showed enhanced activity against *S. aureus* across multiple concentrations (0.05%, 1%, and up to 5%) compared to control. In contrast, no significant antimicrobial activity was recorded against *Pseudomonas* sp. across all samples, indicating inherent resistance. The findings suggest that samples containing varying concentrations exhibit differing degrees of antimicrobial efficacy against specific bacterial strains. Notably, samples containing higher concentrations demonstrated enhanced inhibitory effects against *Staphylococcus aureus* and *Escherichia coli*, while showing limited effectiveness against *Pseudomonas* sp. The results obtained warrant further investigations to explore potential applications of these compounds to be used as antimicrobials and also to design newer molecules with better functionality Figure 7.

Contact Angle of HNTs-Acephate Emulsion on the Leaf Surface—The spreading, wetting, and adhesion behavior of pesticide formulations on plant leaves are all influenced by the contact angle. The contact angle plays a major role in determining the droplet wettability of a leaf surface. The droplet's wettability can be classified as good ($\theta < 60^\circ$), moderate ($60^\circ \leq \theta < 80^\circ$), poor ($80^\circ \leq \theta < 100^\circ$), or very poor ($\theta \geq 100^\circ$). The higher the contact angle of the droplet on the leaf surface, the less wet the liquid will be on that surface. The surface of Maize and cotton leaves were coated with 8 µL of Acephate emulsion containing 0, 0.5, 1, 2, and 5 weight percent HNTs in water in order to assess the wetting properties of the emulsions on the crop leaves. Data Physics, OCA-25, Germany's DSA 100 contact angle analyzer was used to measure the droplet contact angle's magnitude on the leaf surface.

On cotton leaves, an emulsion based on neem oil with a ratio of 2 + 8 ML displays the contact angle trend shown below. Its range of 61.82˚ to 69.08˚ indicates a high degree of wettability. The emulsions with 0.2 and 0.5% HNT concentrations had lower contact angles (61.82˚ & 64.76˚, respectively). In a similar vein, an emulsion with a 7 + 3 ML ratio of water to Neem oil exhibits an irregular contact angle trend. The contact angle first decreases and then slightly increases as the emulsifier concentration rises. The contact angles of the emulsions with 0.05 and 0.2% HNT concentrations were lower than those of the others (48.62˚ and 56.56˚, respectively). Conversely, an emulsion with a 9 + 1 ML ratio of water to Neem oil exhibits exceptional wettability on cotton leaves due to a contact angle that falls between 58.82˚ and 50.07˚. The contact angles of the emulsions containing 0.05 and 0.5% HNT concentrations were lower than those of the others (51.06˚ and 50.07˚, respectively). When the contact angle for cotton leaves is compared, the maize leaves perform better. A Pickering emulsion based on neem oil with a proportion of 8 + 2 ML exhibits excellent wettability. As the concentration of emulsifier HNT increases, the contact angle decreases. Its location ranges from 48.09˚ to 29.0˚. The emulsion with the shortest contact angle and the best hydrophilic nature is the 0.5% concentration. The contact angle for Pickering emulsions with

an oil to water ratio of 3 + 7 and 1 + 9 falls between 58˚ and 61˚. For both kinds of emulsions, the contact angle shows an irregular trend. However, contact angle on maize leaves shows a modest degree of wettability. The contact angle for different concentrations of neem oil-based emulsion on cotton and maize leaves is displayed in Figures 8-13.

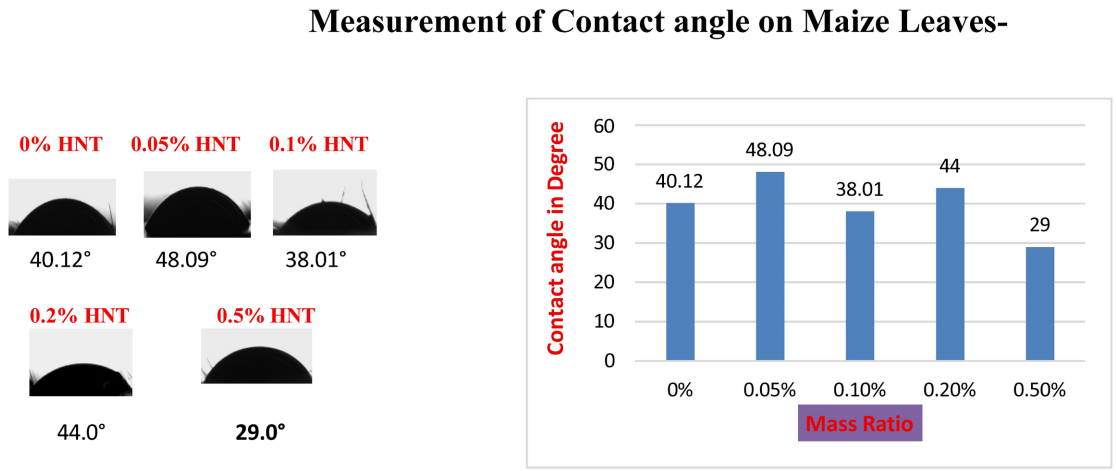

Figure 8. Contact angle of Neem oil-based Pickering emulsion on Maize leaves with the proportion (8 + 2 ML).

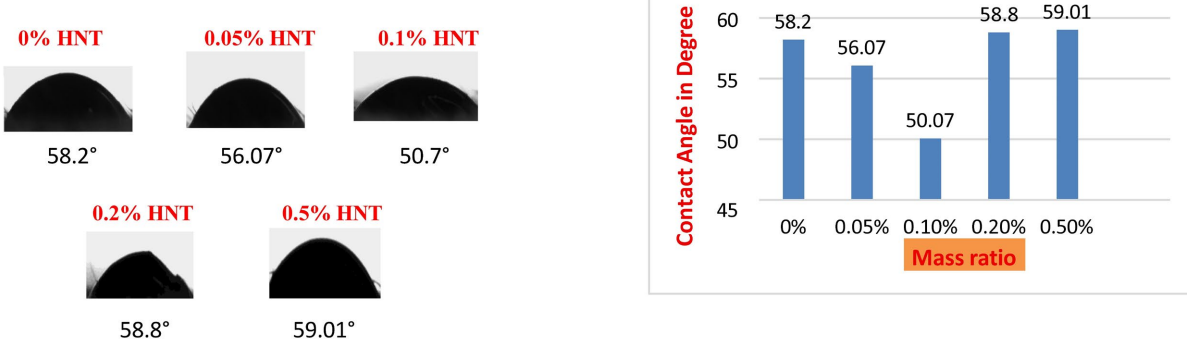

Figure 9. Contact angle of Neem oil-based Pickering emulsion on Maize leaves with the proportion (7 + 3 ML).

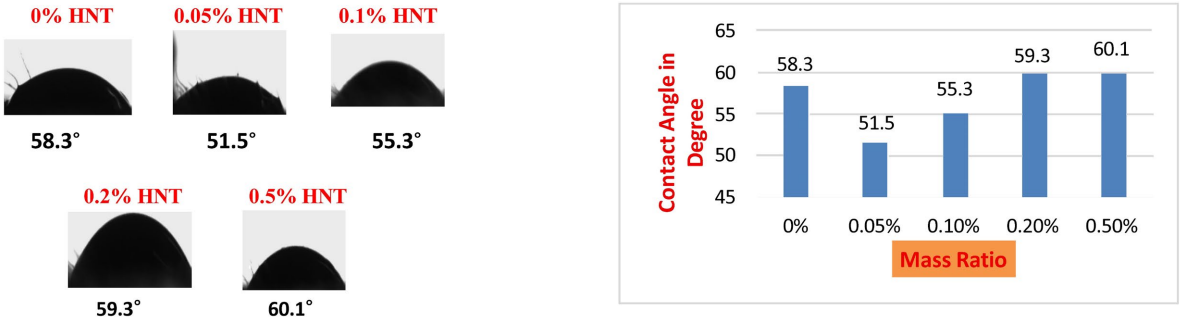

Figure 10. Contact angle of Neem oil-based Pickering emulsion on Maize leaves with the proportion (9 + 1 ML).

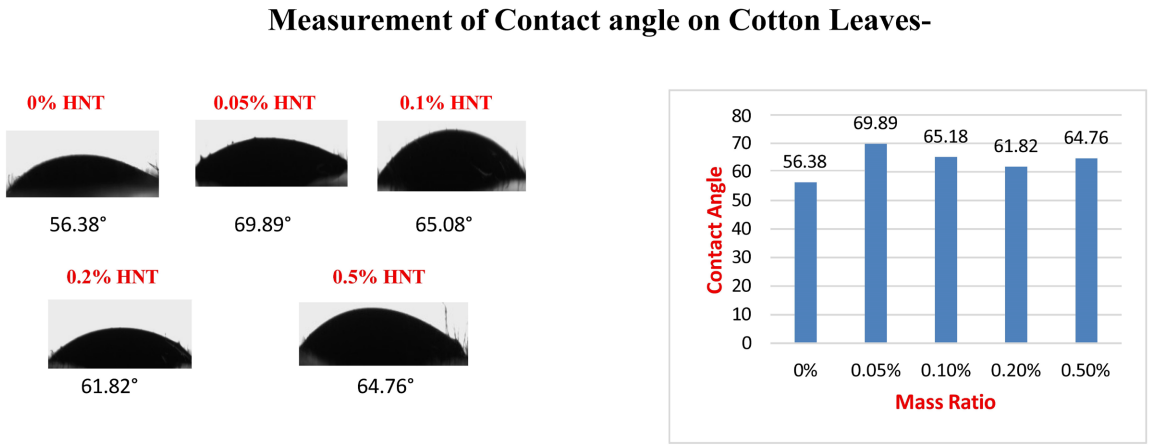

Figure 11. Contact angle of Neem oil-based Pickering emulsion on Cotton leaves with the proportion (8 + 2 ML).

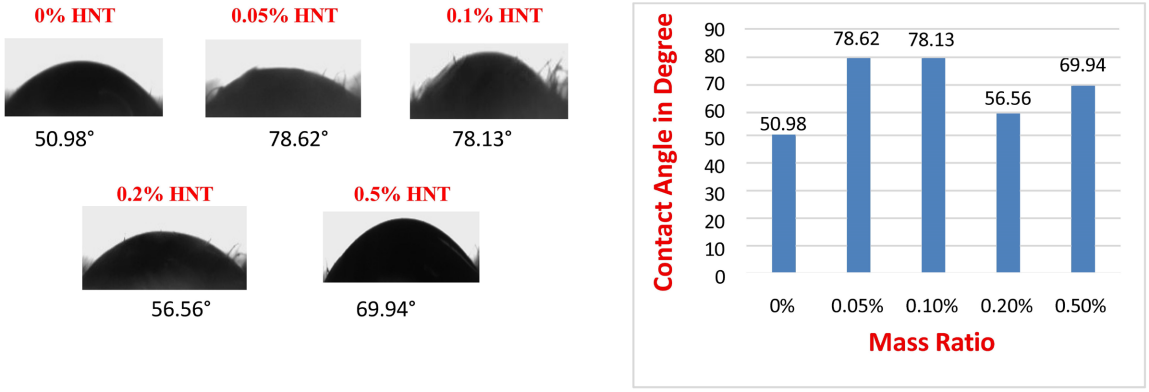

Figure 12. Contact angle of Neem oil-based Pickering emulsion on Cotton leaves with the proportion (7 + 3 ML).

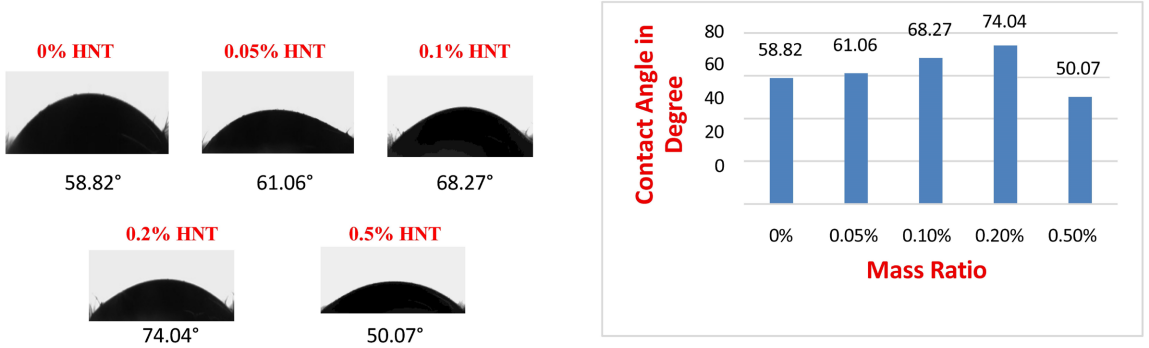

Figure 13. Contact angle of Neem oil-based Pickering emulsion on Cotton leaves with the proportion (9 + 1 ML).

FTIR Analysis

Fourier transform infrared (FTIR) spectroscopy was used to confirm the successful fabrication of the neem oil-based Pickering emulsion stabilized by halloysite nanotubes (HNTs) and loaded with acephate. Figure 14 describes the FTIR Analysis for Neem oil-based Pickering emulsion.

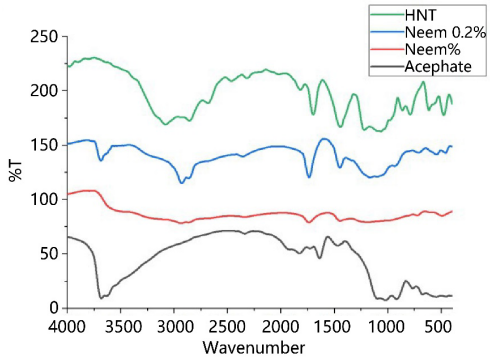

Figure 14. FTIR analysis for Neem oil-based Pickering emulsion.

The FTIR spectrum of HNT exhibited characteristic aluminosilicate bands. The sharp absorption peaks observed at 3695 - 3620 cm^{-1} correspond to the stretching vibrations of inner surface Al-OH groups, confirming the structural hydroxyl groups of halloysite. A broad band centered around 3450 - 3200 cm^{-1} is attributed to hydrogen-bonded O-H stretching of adsorbed water molecules [5] [24]-[27]. The band near 1630 cm^{-1} corresponds to H-O-H bending vibrations of interlayer water. A strong and prominent band in the region of 1080 - 1030 cm^{-1} is assigned to Si-O-Si stretching vibrations, which is the fingerprint region of aluminosilicate frameworks. Additionally, the band at ~910 cm^{-1} is due to Al-OH bending, while bands below 600 cm^{-1} correspond to Si-O and Al-O lattice vibrations. These results confirm the structural integrity of the halloysite nanotubes after formulation.

Neem oil showed characteristic lipid absorption bands. The peaks at ~2925 and ~2855 cm^{-1} correspond to asymmetric and symmetric stretching vibrations of aliphatic -CH_2 groups, confirming the presence of long hydrocarbon chains. The intense band at ~1740 cm^{-1} is attributed to the C=O stretching vibration of ester groups present in triglycerides. Additional bands at 1465 - 1375 cm^{-1} arise from CH_2 bending and CH_3 deformation vibrations. The peaks observed in the range of 1240 - 1160 cm^{-1} correspond to C-O stretching of ester linkages. An increase in the intensity of these characteristic peaks with higher neem concentration confirms the proportional increase of the oil phase in the emulsion system.

The spectrum of acephate displayed distinct absorption bands characteristic of organophosphate compounds. The band observed around 1650 cm^{-1} is attributed to amide C=O stretching, while peaks in the region of 1250 - 1020 cm^{-1} correspond to P=O and P-O-C stretching vibrations. The presence of bands near 650 - 560 cm^{-1} is associated with P-S stretching vibrations of the phosphorothioate group. These peaks confirm the structural identity of acephate.

In the formulated Pickering emulsion system, characteristic peaks corresponding to HNT (Si-O-Si and Al-OH), neem oil (C-H and ester C=O), [28]-[31] and acephate (amide and phosphate groups) were retained, indicating the successful incorporation of all components. Notably, slight broadening of the O-H stretching band and minor shifts in the carbonyl and phosphate regions were observed, suggesting hydrogen bonding interactions between the surface hydroxyl groups of HNT and the functional groups of neem oil and acephate. The strong Si-O band of

HNT partially overlaps with the P-O-C stretching of acephate, indicating possible adsorption or confinement within the nanotube lumen or at the oil-water interface.

Importantly, no new absorption bands were detected, indicating the absence of covalent bond formation and confirming that the encapsulation process is primarily physical in nature. The results demonstrate that acephate is successfully loaded within the HNT-stabilized neem oil Pickering emulsion through adsorption and interfacial stabilization mechanisms without altering the chemical structure of the individual components.

Overall, FTIR analysis confirms the successful preparation of a neem oil-based Pickering emulsion stabilized by halloysite nanotubes and effectively loaded with acephate, with evidence of intermolecular interactions contributing to system stability.

The three-dimensional structure of the freeze-dried emulsion droplets was investigated by SEM. Figure 15 is the images for Neem oil Pickering emulsion without emulsifier, it shows that droplets are irregularly shaped and partially merged, which indicates droplet coalescence, and boundaries between droplets are not sharply defined. Surface of droplets appears rough and disrupted, suggesting instability in the emulsion. The Instability of emulsion may be due to absence of emulsifier or may be due to deformation of droplets. While SEM images with presence of emulsifier HNT (Figure 16) shows that particles are spherical, well defined and uniform in size and shape. Which shows that no coalescence or deformation occurs. Emulsifier HNT adsorbs at oil/water interface by capillary forces and covers oil droplets and prevents them from coalescing. The boundary between droplets and surrounding phase appears sooth and well defined. A more stable emulsion with well-maintained droplet integrity and dispersion is depicted in this image.

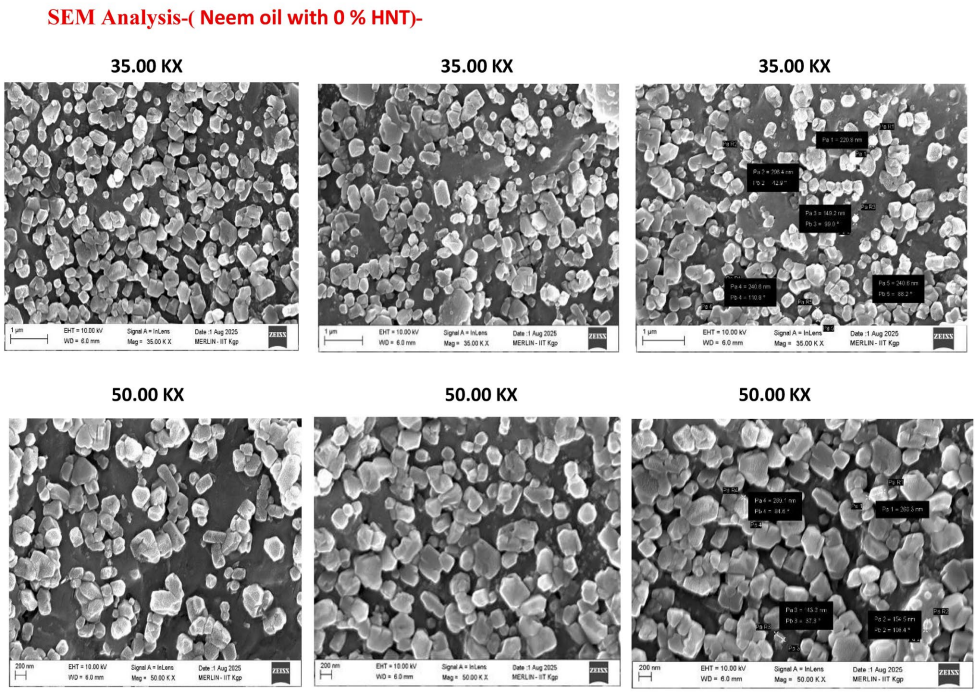

Figure 15. SEM images with 0% HNT.

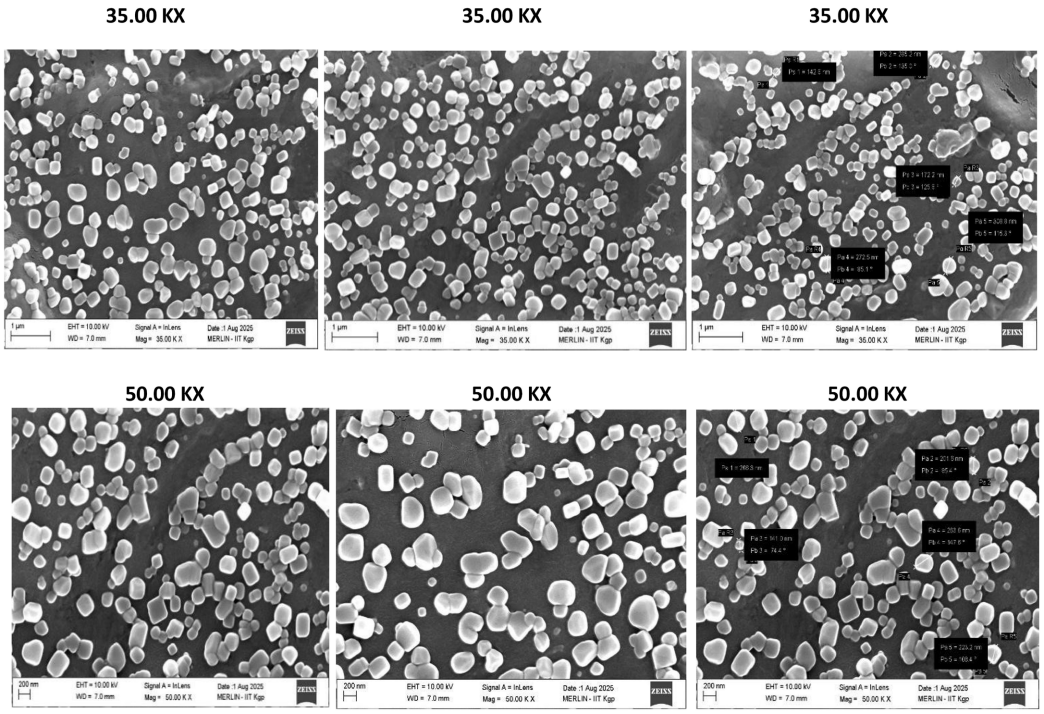

Figure 16. SEM images with 0.2 % HNT.

EDS Analysis -

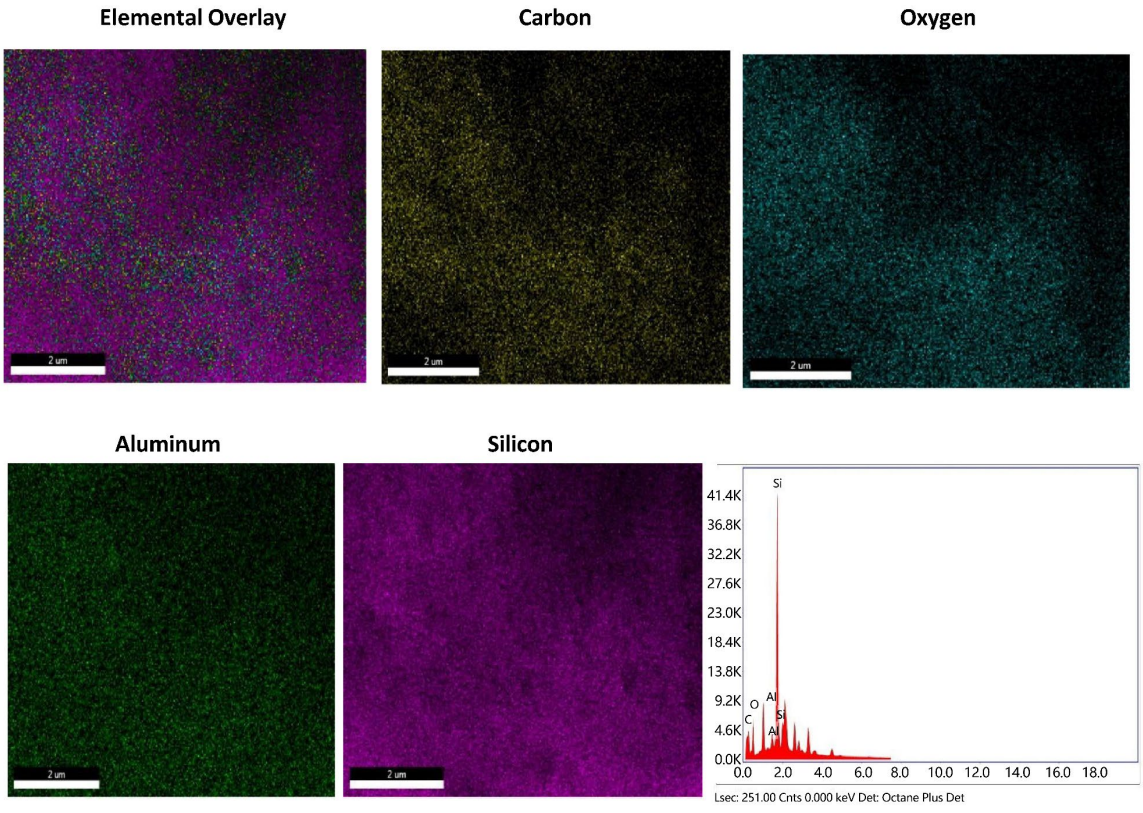

Figure 17. EDS analysis of Neem oil with 0% HNT.

Table 4. Elemental analysis of Neem oil with 0% HNT.

Element	Weight %	Atomic %	Net Int.	Error %	Kratio	Z	R	A	F
C K	48.64	63.85	390.9	9.63	0.10	1.06	0.97	0.19	1.00
O K	17.18	16.93	293	9.51	0.04	1.01	0.99	0.22	1.00
AlK	1.56	0.91	141.8	4.10	0.01	0.89	1.03	0.88	1.04
SiK	32.62	18.31	2928.7	2.10	0.28	0.91	1.03	0.94	1.00

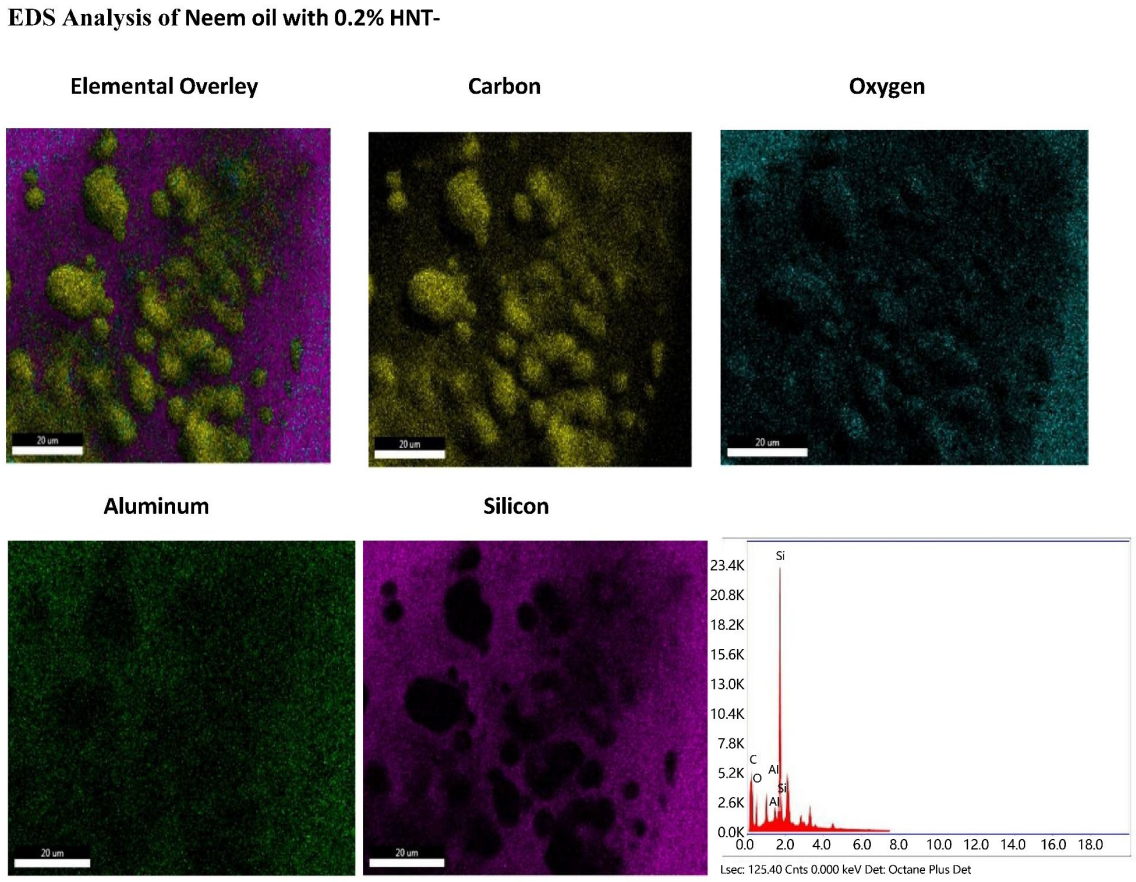

Figure 18. EDS analysis of Neem oil with 0.2% HNT.

Table 5. Elemental analysis of Neem oil with 0.2% HNT.

Element	Weight %	Atomic %	Net Int.	Error %	Kratio	Z	R	A	F
C K	59.27	72.78	899.8	9.10	0.15	1.04	0.98	0.24	1.00
O K	14.62	13.48	340.1	10.02	0.03	0.99	1.00	0.20	1.00
AlK	1.38	0.75	186.7	4.40	0.01	0.88	1.03	0.89	1.03
SiK	24.74	12.99	3328.5	2.13	0.21	0.89	1.04	0.94	1.00

The EDS data show a clear compositional shift when halloysite nanotubes are used as an emulsifier. The neem-oil emulsion without emulsifier exhibits 32.6 wt% Si and 48.6 wt% C, (Shown in **Table 4**) whereas the halloysite-stabilized emulsion

shows a marked increase in carbon (59.3 wt%) and a concurrent decrease in silicon (24.7 wt%) and oxygen. (Shown in **Table 5**). The dominance of the Si peak in both spectra indicates the presence of aluminosilicate material, but the reduced relative Si (and O) signal in the halloysite-containing formulation, together with the higher surface C fraction, suggests a thicker organic overlayer or greater surface coverage of oil/organics on halloysite particles in that sample [32]-[34]. In other words, halloysite nanotubes appear to be well incorporated into the organic phase and covered/coated by the neem oil/acephate matrix, attenuating the detectable Si signal from the particle surface. The small change in Al is consistent with a low absolute Al content and is within typical measurement uncertainty for light Al signals in organic matrices. Overall, the EDS images (**Figure 17** & **Figure 18**) and results are consistent with halloysite acting as a Pickering-type stabilizer that is embedded within or coated by the organic phase, which should enhance interfacial stabilization of droplets compared to the formulation without emulsifier [35]-[38].

Insecticidal Activity:

Spodoptera frugiperda is commonly known as the fall armyworm. It is polyphagous lepidopteran pest which has become a significant threat to agricultural industry all over the globe. Its aggressive feeding behavior during larval stage causes extensive foliar damage, whorl tissue destruction, [38]-[41] and compromised reproductive structures. It also affects photosynthetic efficiency and plant Vigor. *Spodoptera frugiperda* mainly attacks on plants like Maize, Cotton, Sorghum, rice, sugarcane etc. It has an ability to develop resistance to multiple classes of insecticides [42]-[48]. So, it is essential to create alternative, environmentally friendly pest management techniques because of the negative effects linked to *S. frugiperda*. Neem oil is an organic pesticide. Its Pickering emulsions are created using water and the insecticide acephate; HNTs stabilize these emulsions. The insecticidal activity of neem oil-based Pickering emulsions was evaluated against larvae of *Spodoptera frugiperda* using a standard leaf-dip method [49]-[53]. Fresh maize leaves were washed with distilled water and air-dried. Leaves were dipped into respective Pickering emulsions containing varying concentrations of neem oil and HNT-acephate formulations for 30 s and air-dried at room temperature. Each treatment consisted of 10 larvae per replicate, with three independent replicates (n = 30 larvae per treatment). **Figure 19** illustrates how treated leaves were put in Petri dishes and how the larvae were left to feed for 24 hours in a controlled laboratory setting (27 ± 2˚C; 65 ± 5% relative humidity).

Controls Negative control: Distilled water-treated leaves**, Positive control:** Commercial acephate formulation (0.1%).

Larvae were considered dead if no movement was observed upon gentle probing. **Table 6** and **Table 7** demonstrates the Mortality (%) of *Spodoptera frugiperda* larvae after 24 h exposure to Pickering emulsions. Sample B (2:8 O/W ratio) demonstrated significantly higher larval mortality (86.7 ± 3.1^{c} %) compared to Sample A (68.3 ± 2.5^{b} %) and Sample C (52.1 ± 3.8^{a} %). No mortality was observed in the negative control (distilled water-treated leaves), confirming that larval

death was attributable to the treatment formulations. The positive control (commercial acephate 0.1%) exhibited 96.2 ± 1.4^{d} % mortality.

These findings indicate that the 2:8 O/W ratio provides optimal dispersion and bioavailability of active ingredients, leading to enhanced insecticidal efficacy. Larval mortality increased significantly with increasing concentration of halloysite nanotubes (HNTs). Emulsions containing 0.5% HNT exhibited the highest mortality (91.4 ± 2.2^{c} %), followed by 0.2% HNT (84.6 ± 2.8^{b} %). Treatments with 0.1% and 0% HNT showed significantly lower mortality (61.5 ± 3.3^{a} % and 49.8 ± 4.0^{a} %, respectively) ($p < 0.05$). This suggests that higher emulsifier concentration enhances formulation stability and improves sustained release of neem oil and acephate.

Table 6. Mortality (%) of *Spodoptera frugiperda* larvae after 24 h exposure to Pickering emulsions.

Treatment	Mortality (%) (Mean ± SD)
Negative Control (Water)	0.0 ± 0.0^{a}
Sample A (3:7)	68.3 ± 2.5^{b}
Sample B (2:8)	86.7 ± 3.1^{c}
Sample C (1:9)	52.1 ± 3.8^{a}
Positive Control (Acephate 0.1%)	96.2 ± 1.4^{d}

Table 7. Effect of HNT concentration on larval mortality Insecticidal Bioassay.

HNT (%)	Mortality (%) (Mean ± SD)
0.0	49.8 ± 4.0^{a}
0.1	61.5 ± 3.3^{a}
0.2	84.6 ± 2.8^{b}
0.5	91.4 ± 2.2^{c}

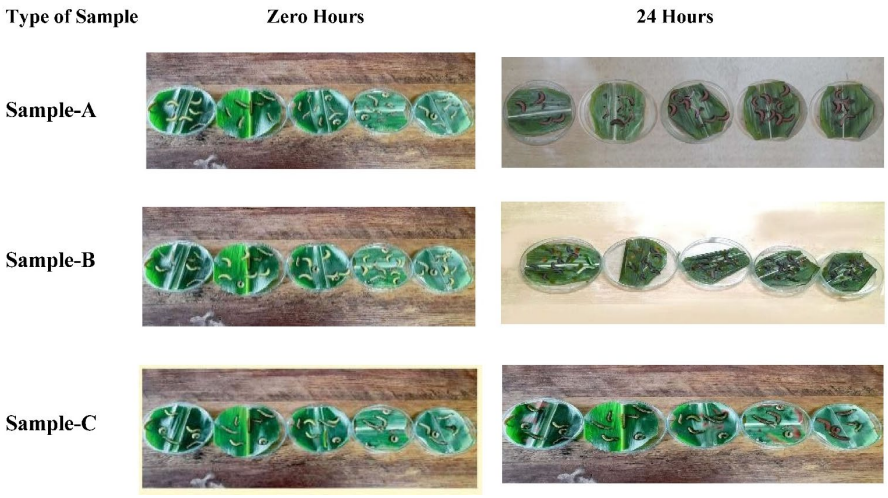

Figure 19. Larval mortality Insecticidal Bioassay.

3. Result and Conclusion

In this study, Pickering emulsions with varying concentrations are made using neem oil. Acephate was added to test the insecticidal properties, and halloysite nano clay is added as a stabilizing agent. The Pickering emulsion with a 2:8 oil-water ratio shows better stability and smaller droplets at HNT concentrations of 0.2% and 0.5%, according to microscopic images of the prepared emulsions. The sample with 0.2% HNT has the smallest droplet size and the highest stability out of all these samples. Consequently, the interfacial tension and droplet size decrease as the HNT concentration rises. Cotton and maize leaves were used to measure the contact angle. When compared to cotton leaves, maize leaves exhibit superior performance in terms of contact angle. Excellent wettability is demonstrated by a Pickering emulsion based on neem oil with a ratio of 2 + 8 Ml. The contact angle falls as the emulsifier HNT concentration rises. The range of its location is 48.09˚ to 29.0˚. The emulsions at concentrations of 0.2% and 0.5% have the shortest contact angle and the best hydrophilic properties. The FTIR spectrum reveals a stable Pickering emulsion in which the physical interactions of halloysite nanotubes (HNTs) effectively stabilize the Neem oil-water interface, enhancing resistance to coalescence and sedimentation. Stable Pickering emulsions are distinguished by the effective adsorption of HNTs on the droplet interface, which is confirmed by the SEM images. These structural characteristics are expected to provide the system with exceptional morphological stability. The effects of different HNTs-acephate emulsion concentrations on the bacteria *Staphylococcus aureus*, *Bacillus cereus*, *Pseudomonas* sp., and *Escherichia coli* were examined in order to evaluate the biosafety of these emulsions. The results imply that samples with different concentrations show various levels of antibacterial activity against particular species of bacteria. Interestingly, samples with higher concentrations showed limited efficacy against *Pseudomonas* sp. but improved inhibitory effects against *Staphylococcus aureus* and *Escherichia coli*. The insecticidal activity of HNTs-Acephate emulsions was evaluated using maize as the plant model and *S. frugiperda* as the pest model. All experimental treatment groups' mortality rates were completed within 24 hours, according to the experimental results. Sample C (1:9 oil-water ratio) has the lowest mortality rate, while sample A (3:7 oil-water ratio) has a moderate one. The highest mortality rate is found in Sample B (2:8 oil-water ratio). The mortality rate is highest in emulsions with 0.5 and 0.2% HNT and lowest in those with 0.0 and 0.1 percent HNT. We conclude from this study that the stability of the emulsion and the mortality rate both rise as the percentage of emulsifier increases.

The stability of the emulsions was visually and microscopically monitored over a period of 15 days at ambient storage conditions (25˚C ± 2˚C). Additionally, to observe potential phase separation under variable environmental conditions, samples were also stored at 4˚C (refrigeration) and 40˚C (elevated temperature) for 15 days. Visual observations for creaming, coalescence, or phase separation were recorded at regular intervals. "Thermal cycling between 4˚C and 45˚C confirmed the robustness of the HNT interfacial film against coalescence."

Funding

This work was supported by the Vice Chancellor research motivation scheme (VCRMS) conducted by Kavayitri Bahinabai Chaudhari North Maharashtra University Jalgaon (MS) India.

Conflicts of Interest

The authors declare that none of the work described in this paper could have been influenced by any known competing financial interests or personal relationships.

References

[1] Wei, H., Wang, H., Chu, H. and Li, J. (2019) Preparation and Characterization of Slow-Release and Water-Retention Fertilizer Based on Starch and Halloysite. *International Journal of Biological Macromolecules*, **133**, 1210-1218. https://doi.org/10.1016/j.ijbiomac.2019.04.183

[2] Shen, Y., Wang, H., Li, W., Liu, Z., Liu, Y., Wei, H., *et al.* (2020) Synthesis and Characterization of Double-Network Hydrogels Based on Sodium Alginate and Halloysite for Slow Release Fertilizers. *International Journal of Biological Macromolecules*, **164**, 557-565. https://doi.org/10.1016/j.ijbiomac.2020.07.154

[3] Wang, C., He, Z., Liu, Y., Zhou, C., Jiao, J., Li, P., *et al.* (2020) Chitosan-Modified Halloysite Nanotubes as a Controlled-Release Nanocarrier for Nitrogen Delivery. *Applied Clay Science*, **198**, Article 105802. https://doi.org/10.1016/j.clay.2020.105802

[4] El Assimi, T., Chaib, M., Raihane, M., El Meziane, A., Khouloud, M., Benhida, R., *et al.* (2020) Poly(ε-Caprolactone)-G-Guar Gum and Poly(ε-Caprolactone)-G-Halloysite Nanotubes as Coatings for Slow-Release DAP Fertilizer. *Journal of Polymers and the Environment*, **28**, 2078-2090. https://doi.org/10.1007/s10924-020-01750-7

[5] Masoudniaragh, A., Oraei, M., Gohari, G., Akbari, A. and Faramarzi, A. (2021) Using Halloysite Nanotubes as Carrier for Proline to Alleviate Salt Stress Effects in Sweet Basil (*Ocimum basilicum* L.). *Scientia Horticulturae*, **285**, Article 110202. https://doi.org/10.1016/j.scienta.2021.110202

[6] Yaakov, N., Ananth Mani, K., Felfbaum, R., Lahat, M., Da Costa, N., Belausov, E., *et al.* (2018) Single Cell Encapsulation via Pickering Emulsion for Biopesticide Applications. *ACS Omega*, **3**, 14294-14301. https://doi.org/10.1021/acsomega.8b02225

[7] Li, J., Cheng, M., Yang, C., Zhang, Y. and Li, D. (2022) Regenerated Cellulose-Stabilized Pickering Emulsion for Sustained Release of Imidacloprid. *Colloid and Polymer Science*, **300**, 1169-1177. https://doi.org/10.1007/s00396-022-05017-6

[8] Ramadhany, P., Witono, J.R.B. and Rosaria, R. (2021) Neem-Based Oil-in-Water (O/W) Emulsion as a Biopesticide. *IOP Conference Series: Materials Science and Engineering*, **1053**, Article 012047. https://doi.org/10.1088/1757-899x/1053/1/012047

[9] Chen, L., Huang, J., Chen, J., Shi, Q., Chen, T., Qi, G., *et al.* (2022) Halloysite Nanotube-Based Pesticide Formulations with Enhanced Rain Erosion Resistance, Foliar Adhesion, and Insecticidal Effect. *ACS Applied Materials & Interfaces*, **14**, 41605-41617. https://doi.org/10.1021/acsami.2c11234

[10] Yuan, P., Tan, D. and Annabi-Bergaya, F. (2015) Properties and Applications of Halloysite Nanotubes: Recent Research Advances and Future Prospects. *Applied Clay Science*, **112**, 75-93. https://doi.org/10.1016/j.clay.2015.05.001

[11] Lisuzzo, L., Cavallaro, G., Milioto, S. and Lazzara, G. (2022) Pickering Emulsions Stabilized by Halloysite Nanotubes: From General Aspects to Technological Applications. *Advanced Materials Interfaces*, **9**, Article 2102346. https://doi.org/10.1002/admi.202102346

[12] Cui, Y., Threlfall, M. and van Duijneveldt, J.S. (2011) Optimizing Organoclay Stabilized Pickering Emulsions. *Journal of Colloid and Interface Science*, **356**, 665-671. https://doi.org/10.1016/j.jcis.2011.01.046

[13] Zhong, B., Wang, S., Dong, H., Luo, Y., Jia, Z., Zhou, X., *et al.* (2017) Halloysite Tubes as Nanocontainers for Herbicide and Its Controlled Release in Biodegradable Poly(Vinyl Alcohol)/Starch Film. *Journal of Agricultural and Food Chemistry*, **65**, 10445-10451. https://doi.org/10.1021/acs.jafc.7b04220

[14] Wang, S., Jia, Z., Zhou, X., Zhou, D., Chen, M., Xie, D., *et al.* (2017) Preparation of a Biodegradable Poly(Vinyl Alcohol)-Starch Composite Film and Its Application in Pesticide Controlled Release. *Journal of Applied Polymer Science*, **134**, Article 45051. https://doi.org/10.1002/app.45051

[15] Yang, J., Zang, W., Zhang, Z., Wang, P. and Yang, Q. (2019) The Enhanced and Tunable Sustained Release of Pesticides Using Activated Carbon as a Carrier. *Materials*, **12**, Article 4019. https://doi.org/10.3390/ma12234019

[16] Tan, D., Yuan, P., Annabi-Bergaya, F., Liu, D. and He, H. (2015) Methoxy-Modified Kaolinite as a Novel Carrier for High-Capacity Loading and Controlled-Release of the Herbicide Amitrole. *Scientific Reports*, **5**, Article 8870. https://doi.org/10.1038/srep08870

[17] Tan, D., Yuan, P., Annabi-Bergaya, F., Dong, F., Liu, D. and He, H. (2015) A Comparative Study of Tubular Halloysite and Platy Kaolinite as Carriers for the Loading and Release of the Herbicide Amitrole. *Applied Clay Science*, **114**, 190-196. https://doi.org/10.1016/j.clay.2015.05.024

[18] Wang, X., Hou, X., Zou, P., Huang, A., Zhang, M. and Ma, L. (2022) Cationic Starch Modified Bentonite-Alginate Nanocomposites for Highly Controlled Diffusion Release of Pesticides. *International Journal of Biological Macromolecules*, **213**, 123-133. https://doi.org/10.1016/j.ijbiomac.2022.05.148

[19] Wang, K., Sun, X., Long, B., Li, F., Yang, C., Chen, J., *et al.* (2021) Green Production of Biodegradable Mulch Films for Effective Weed Control. *ACS Omega*, **6**, 32327-32333. https://doi.org/10.1021/acsomega.1c05725

[20] Zeng, X., Zhong, B., Jia, Z., Zhang, Q., Chen, Y. and Jia, D. (2019) Halloysite Nanotubes as Nanocarriers for Plant Herbicide and Its Controlled Release in Biodegradable Polymers Composite Film. *Applied Clay Science*, **171**, 20-28. https://doi.org/10.1016/j.clay.2019.01.021

[21] Meyer, W.L., Gurman, P., Stelinski, L.L. and Elman, N.M. (2015) Functional Nano-Dispensers (FNDs) for Delivery of Insecticides against Phytopathogen Vectors. *Green Chemistry*, **17**, 4173-4177. https://doi.org/10.1039/c5gc00717h

[22] Seven, S.A., Tastan, Ö.F., Tas, C.E., Ünal, H., Ince, İ.A. and Menceloglu, Y.Z. (2019) Insecticide-releasing LLDPE Films as Greenhouse Cover Materials. *Materials Today Communications*, **19**, 170-176. https://doi.org/10.1016/j.mtcomm.2019.01.015

[23] Qin, Y., An, T., Cheng, H., Su, W., Meng, G., Wu, J., *et al.* (2022) Functionalized Halloysite Nanotubes as Chlorpyrifos Carriers with High Adhesion and Temperature Response for Controlling of Beet Armyworm. *Applied Clay Science*, **222**, Article 106488. https://doi.org/10.1016/j.clay.2022.106488

[24] El Assimi, T., Lakbita, O., El Meziane, A., Khouloud, M., Dahchour, A., Beniazza, R., *et al.* (2020) Sustainable Coating Material Based on Chitosan-Clay Composite and

Paraffin Wax for Slow-Release DAP Fertilizer. *International Journal of Biological Macromolecules*, **161**, 492-502. https://doi.org/10.1016/j.ijbiomac.2020.06.074

[25] Saki, H., Alemayehu, E., Schomburg, J. and Lennartz, B. (2019) Halloysite Nanotubes as Adsorptive Material for Phosphate Removal from Aqueous Solution. *Water*, **11**, Article 203. https://doi.org/10.3390/w11020203

[26] Vo, P.T., Nguyen, H.T., Trinh, H.T., Nguyen, V.M., Le, A., Tran, H.Q., *et al.* (2021) The Nitrogen Slow-Release Fertilizer Based on Urea Incorporating Chitosan and Poly(Vinyl Alcohol) Blend. *Environmental Technology & Innovation*, **22**, Article 101528. https://doi.org/10.1016/j.eti.2021.101528

[27] Wang, C., Song, S., Yang, Z., Liu, Y., He, Z., Zhou, C., *et al.* (2022) Hydrophobic Modification of Castor Oil-Based Polyurethane Coated Fertilizer to Improve the Controlled Release of Nutrient with Polysiloxane and Halloysite. *Progress in Organic Coatings*, **165**, Article 106756. https://doi.org/10.1016/j.porgcoat.2022.106756

[28] Chen, L., Guo, Z., Lao, B., Li, C., Zhu, J., Yu, R., *et al.* (2021) Phytotoxicity of Halloysite Nanotubes Using Wheat as a Model: Seed Germination and Growth. *Environmental Science*: *Nano*, **8**, 3015-3027. https://doi.org/10.1039/d1en00507c

[29] Yang, Y., Fang, Z., Chen, X., Zhang, W., Xie, Y., Chen, Y., *et al.* (2017) An Overview of Pickering Emulsions: Solid-Particle Materials, Classification, Morphology, and Applications. *Frontiers in Pharmacology*, **8**, Article ID: 235054. https://doi.org/10.3389/fphar.2017.00287

[30] Pang, Y., Wang, S., Qiu, X., Luo, Y., Lou, H. and Huang, J. (2017) Preparation of Lignin/Sodium Dodecyl Sulfate Composite Nanoparticles and Their Application in Pickering Emulsion Template-Based Microencapsulation. *Journal of Agricultural and Food Chemistry*, **65**, 11011-11019. https://doi.org/10.1021/acs.jafc.7b03784

[31] Wu, J. and Ma, G. (2016) Recent Studies of Pickering Emulsions: Particles Make the Difference. *Small*, **12**, 4633-4648. https://doi.org/10.1002/smll.201600877

[32] Shorey, R. and Mekonnen, T.H. (2023) Esterification of Lignin with Long Chain Fatty Acids for the Stabilization of Oil-in-Water Pickering Emulsions. *International Journal of Biological Macromolecules*, **230**, Article 123143. https://doi.org/10.1016/j.ijbiomac.2023.123143

[33] Wang, Y., Li, X., Shen, C., Mao, Z., Xu, H., Zhong, Y., *et al.* (2020) Lignin Assisted Pickering Emulsion Polymerization to Microencapsulate 1-Tetradecanol for Thermal Management. *International Journal of Biological Macromolecules*, **146**, 1-8. https://doi.org/10.1016/j.ijbiomac.2019.12.175

[34] Van Hooghten, R., Blair, V.E., Vananroye, A., Schofield, A.B., Vermant, J. and Thijssen, J.H.J. (2017) Interfacial Rheology of Sterically Stabilized Colloids at Liquid Interfaces and Its Effect on the Stability of Pickering Emulsions. *Langmuir*, **33**, 4107-4118. https://doi.org/10.1021/acs.langmuir.6b04365

[35] Kpogbemabou, D., Lecomte-Nana, G., Aimable, A., Bienia, M., Niknam, V. and Carrion, C. (2014) Oil-in-Water Pickering Emulsions Stabilized by Phyllosilicates at High Solid Content. *Colloids and Surfaces A*: *Physicochemical and Engineering Aspects*, **463**, 85-92. https://doi.org/10.1016/j.colsurfa.2014.09.037

[36] Cai, X., Li, C., Tang, Q., Zhen, B., Xie, X., Zhu, W., *et al.* (2019) Assembling Kaolinite Nanotube at Water/Oil Interface for Enhancing Pickering Emulsion Stability. *Applied Clay Science*, **172**, 115-122. https://doi.org/10.1016/j.clay.2019.02.021

[37] Cavallaro, G., Milioto, S., Nigamatzyanova, L., Akhatova, F., Fakhrullin, R. and Lazzara, G. (2019) Pickering Emulsion Gels Based on Halloysite Nanotubes and Ionic Biopolymers: Properties and Cleaning Action on Marble Surface. *ACS Applied Nano Materials*, **2**, 3169-3176. https://doi.org/10.1021/acsanm.9b00487

[38] Yu, B., Cheng, J., Fang, Y., Xie, Z., Xiong, Q., Zhang, H., *et al.* (2024) Multi-Stimuli-responsive, Topology-Regulated, and Lignin-Based Nano/Microcapsules from Pickering Emulsion Templates for Bidirectional Delivery of Pesticides. *ACS Nano*, **18**, 10031-10044. https://doi.org/10.1021/acsnano.3c11621

[39] Yu, X., Li, X., Ma, S., Wang, Y., Zhu, W. and Wang, H. (2023) Biomass-Based, Interface Tunable, and Dual-Responsive Pickering Emulsions for Smart Release of Pesticides. *Advanced Functional Materials*, **33**, Article 2214911. https://doi.org/10.1002/adfm.202214911

[40] Yang, C., Li, J., Zhang, Y., Wu, C. and Li, D. (2023) A Pesticide Sustained-Release Microcapsule from Cellulose Nanocrystal Stabilized Pickering Emulsion Template. *Journal of Applied Polymer Science*, **140**, e53716. https://doi.org/10.1002/app.53716

[41] Tang, C., Li, Y., Pun, J., Mohamed Osman, A.S. and Tam, K.C. (2019) Polydopamine Microcapsules from Cellulose Nanocrystal Stabilized Pickering Emulsions for Essential Oil and Pesticide Encapsulation. *Colloids and Surfaces A*: *Physicochemical and Engineering Aspects*, **570**, 403-413. https://doi.org/10.1016/j.colsurfa.2019.03.049

[42] Pang, Y., Li, X., Wang, S., Qiu, X., Yang, D. and Lou, H. (2018) Lignin-Polyurea Microcapsules with Anti-Photolysis and Sustained-Release Performances Synthesized via Pickering Emulsion Template. *Reactive and Functional Polymers*, **123**, 115-121. https://doi.org/10.1016/j.reactfunctpolym.2017.12.018

[43] Kotliarevski, L., Cohen, R., Ramakrishnan, J., Wu, S., Mani, K.A., Amar-Feldbaum, R., *et al.* (2022) Individual Coating of Entomopathogenic Nematodes with Titania (tio_2) Nanoparticles Based on Oil-in-Water Pickering Emulsion: A New Formulation for Biopesticides. *Journal of Agricultural and Food Chemistry*, **70**, 13518-13527. https://doi.org/10.1021/acs.jafc.2c04424

[44] Zou, W., Zhao, Y., Deng, Y., Zhang, H., Mao, Z., Xiong, Y., *et al.* (2022) Preparation of Layered Beta-Cypermethrin-Carrying Microcapsules from Pickering Emulsion of Hollow Mesoporous Silica Nanoparticles. *Materials Today Communications*, **31**, Article 103695. https://doi.org/10.1016/j.mtcomm.2022.103695

[45] Zheng, L., Cheng, X., Cao, L., Chen, Z., Huang, Q. and Song, B. (2022) Enhancing Pesticide Droplet Deposition through O/W Pickering Emulsion: Synergistic Stabilization by Flower-Like ZnO Particles and Polymer Emulsifier. *Chemical Engineering Journal*, **434**, 134761. https://doi.org/10.1016/j.cej.2022.134761

[46] Tian, J., Xie, J., Hao, L., Chen, H., Zhou, X. and Zhou, H. (2024) Zein/Sodium Abietate Complex Stabilized Pickering Emulsion as a Delivery System for Controlled Release of Hydrophobic Photosensitive Pesticide. *Industrial Crops and Products*, **212**, Article 118347. https://doi.org/10.1016/j.indcrop.2024.118347

[47] Yaakov, N., Kottakota, C., Mani, K.A., Naftali, S.M., Zelinger, E., Davidovitz, M., *et al.* (2022) Encapsulation of Bacillus Thuringiensis in an Inverse Pickering Emulsion for Pest Control Applications. *Colloids and Surfaces B*: *Biointerfaces*, **213**, Article 112427. https://doi.org/10.1016/j.colsurfb.2022.112427

[48] Ma, Y., Gao, Y., Zhao, X., Zhu, Y., Du, F. and Hu, J. (2018) A Natural Triterpene Saponin-Based Pickering Emulsion. *Chemistry—A European Journal*, **24**, 11703-11710. https://doi.org/10.1002/chem.201801619

[49] Gan, M., Pan, J., Zhang, Y., Dai, X., Yin, Y., Qu, Q., *et al.* (2014) Molecularly Imprinted Polymers Derived from Lignin-Based Pickering Emulsions and Their Selectively Adsorption of Lambda-Cyhalothrin. *Chemical Engineering Journal*, **257**, 317-327. https://doi.org/10.1016/j.cej.2014.06.110

[50] Zhang, X., Sun, X., Wang, M., Wang, Y., Wu, Q., Ji, L., *et al.* (2020) Dummy Molecularly Imprinted Microspheres Prepared by Pickering Emulsion Polymerization for

Matrix Solid-Phase Dispersion Extraction of Three Azole Fungicides from Fish Samples. *Journal of Chromatography A*, **1620**, Article 461013. https://doi.org/10.1016/j.chroma.2020.461013

[51] Yu, X., Chen, S., Wang, W., Deng, T. and Wang, H. (2022) Empowering Alkali Lignin with High Performance in Pickering Emulsion by Selective Phenolation for the Protection and Controlled-Release of Agrochemical. *Journal of Cleaner Production*, **339**, Article 130769. https://doi.org/10.1016/j.jclepro.2022.130769

[52] Zhou, C., Li, H., Zhou, H., Wang, H., Yang, P. and Zhong, S. (2015) Water-Compatible Halloysite-Imprinted Polymer by Pickering Emulsion Polymerization for the Selective Recognition of Herbicides. *Journal of Separation Science*, **38**, 1365-1371. https://doi.org/10.1002/jssc.201401469

[53] Yin, R., Chen, L. and Ma, L. (2019) Extraction of Matrine from Soil with Matrix Solid-phase Dispersion by Molecularly Imprinted Polymers Derived from Lignin-Based Pickering Emulsions. *Journal of Separation Science*, **42**, 3563-3570. https://doi.org/10.1002/jssc.201900803